

# Synthesis and Characterization of High Solid Content Aqueous Polyurethane Dispersion

Qing-An Li, Dong-Cheng Sun

College of Chemical Science, South China University of Technology, Guangzhou 510640, China

Received 31 October 2005; accepted 12 April 2006

DOI 10.1002/app.24627

Published online 11 May 2007 in Wiley InterScience (www.interscience.wiley.com).

**ABSTRACT:** Aqueous polyurethane (APU) dispersions having a solid content of 50% were synthesized using dimethylol propionic acid (DMPA) as the stabilizing moiety. The principal diols used were poly-1,4-butylene adipate glycol (PBA). The diisocyanates used in this study were a 30:70 blend of hexamethylene diisocyanate (HDI) and isophorone diisocyanate (IPDI). All these samples were neutralized using triethylamine (TEA) and chain-extended using ethylene diamine (EDA). The effects of the COOH content, NCO/OH molar ratio, and molecular weight ( $M_n$ ) of PBA on the properties of APU dispersion and its cast film were studied. Dynamic light scattering results revealed that these high solid content dispersions shown broad particle size distributions as well as bimodal. Differential scanning calorimetry (DSC) and dynamic me-

chanical thermal analysis (DMA) results showed that as the hard segment content increased, the melting point ( $T_m$ ) of the APU cast film increased, but the glass transition temperature ( $T_g$ ) did not show significant alteration, when a PBA lower than 1000  $M_n$  was used, the APU exhibited faint soft-segment crystallization and tended to form amorphous polymer. Tensile and T-peel strength tests attained excellent mechanical properties, such as a maximum Young's modulus of 166 MPa and the elongation at break reached to 2000%. T-peel strength test (PVC/PVC) yielded a maximum peel strength value of 8.8 N/mm. © 2007 Wiley Periodicals, Inc. *J Appl Polym Sci* 105: 2516–2524, 2007

**Key words:** aqueous polyurethane; high solid content; crystallization; particle size distribution

## INTRODUCTION

Aqueous polyurethane (APU), which is note for its versatile application properties and friendly to environment, has become a hotspot for many years. With the rapid development of industry, environmental and legislative pressures, huge quantities of aqueous polyurethane dispersions are demanded each year for a wide variety of uses, such as coatings, adhesives, ink and related end uses. It is reasonable that high solid content dispersions are of growing interest since it will make product transport more efficient and less costly. In addition, a reduction in the water content allows us to reduce film-formation and drying time. Not only does this make applications more efficient, it also reduces energy load needed in some cases.<sup>1–5</sup>

However, in most of the previous researches, the solid content of aqueous polyurethane only ranges from 20 to 35%. It is difficult in making APU with high solid content much above 50 or 60% as the viscosity is highly sensitive to solid content. It is also impossible to predict how many complex factors will affect the viscosity near to upper limit of solids con-

tent. No surprisingly, there are not a significant number of papers available in the open literature that describe the synthesis of high solid content aqueous polyurethane, and most of the work published on this subject seem to be in the patent literature.<sup>6–9</sup>

In this study, high solid content aqueous polyurethane dispersions with low viscosity were prepared by using the well-known prepolymer process. The structure–properties relationship of this high solid content dispersion and their cast films was also investigated.

## EXPERIMENTAL

### Materials

Isophorone diisocyanate (IPDI) and hexamethylene diisocyanate (HDI) were from Bayer (Germany). Poly-1,4-butylene adipate glycol(PBA) with different molecular weight ( $M_n = 1000; 2000; 3000$ ) was a gift of Dong-Guan HonTex Chemical Co. Ltd (China). Dimethylol propionic acid (DMPA) was purchased from Degussa Co. (Shanghai, China). Triethylamine (TEA) and ethylene diamine (EDA) were obtained from RuiJinTe Chemical Co. (Tianjin, China). Acetone and dibutyltin dilaurate (DBTDL) were purchased from BaiShi Chemical Co. (TianJin, China) and TianJin Chemical Reagents Factory (China) respectively. All these materials were used without further purification.

Correspondence to: D.-C. Sun (chdcun@scut.edu.cn).

### Preparation of the APU dispersions

The synthesis of the prepolymer based on PBA, DMPA, HDI, and IPDI, catalyzed by DBTDL, was carried out in the presence of appropriate amount of acetone in N<sub>2</sub> atmosphere. The mixture was reacted at 75°C until the theoretical NCO content of the prepolymer was reached, as determined by the di-*n*-butylamine titration method. The mixture was cooled to 50°C and TEA was added. The neutralization reaction was proceeded at the same temperature for 30 min. The prepolymer was then brought down to room temperature and dispersed in water (based on 50% solid content) under vigorous stirring. Afterward, EDA was added to the dispersion and the temperature was kept at 50°C for about 40 min to complete the chain-extension reaction between the amino groups of the chain extender and the NCO end groups of the prepolymer. A finely divided dispersion was obtained after acetone was distilled off.

### Characterization

#### Viscosity

The viscosities of the APU dispersion were measured in a Brookfield digital viscometer (Model DV-II). Measurements were carried out at 25°C, by using the spindle No.1 at 30 rpm.

#### Particle size distribution analysis

The particle size and its distribution of the dispersions were analyzed by dynamic light scattering (7032 Multi-8 with wavelength of 633 nm, Malvern Instrument Co., England). This procedure involved diluting a few drops of the dispersion in distilled deionized water to an approximate concentration of 0.1% and was then measured at 25°C.

#### Transmission electron microscope analysis

State of dispersion was investigated by transmission electron microscopy (TEM, FEI-Tecnaï 12). To obtain the micrographs, the samples were stained with OsO<sub>4</sub>.

#### Tensile test

The tensile properties of the cast films were measured at room temperature using an Instron 5566 testing machine, according to the ASTM D-412 specifications. A crosshead speed of 100 mm/min was used.

#### T-peel strength test

As per the ASTM-D1876 requirements, peel strength was determined by applying the synthesized APU

dispersion with a brush to both pieces of fiber-intensified PVC (polyvinyl chloride) to a thickness of 0.1 mm, the two layers were dried at 70°C and placed together. A load of about 1 kg was placed on the joint and kept over there for 24 h. Then, the PVC joints were conditioned at room temperature (30°C) for 7 days. Test specimens were cut into strips to form an area of overlap measuring 2.5 × 20 cm<sup>2</sup>. These PVC joints were subjected to lap shear tests on an Instron 5566 testing machine with a head speed of 200 mm/min.

#### Differential scanning calorimetry

Differential scanning calorimetry (DSC) was carried out over a temperature range from room temperature to 200°C using a Du Pont 600 DSC at a heating rate of 10°C/min under nitrogen purging.

#### Dynamic mechanical thermal analysis

Dynamic mechanical thermal analysis (DMA) was carried out on a DMA 242 (Netzsch, Germany) in tension mode, over a temperature range from -100°C to 150°C at a frequency of 10 Hz and a heating rate of 5°C/min. The size of the specimens prepared was 1.5 × 0.4 × 0.1 cm<sup>3</sup>.

## RESULTS AND DISCUSSION

### Viscosity, particle size, and particle size distribution of APU dispersions

Three series of APU dispersions were prepared by varying the DMPA content, NCO/OH molar ratio, and *M<sub>n</sub>* of PBA respectively, (Table I). It was found that with a high solid content up to 50%, the synthesized APU samples still had low viscosity (<1500 mp s) and good storage stability, except APU1085. It is known that the viscosity of APU is highly sensitive to particle size and particle size distribution (PSD). Smaller particle size and narrower PSD usually result in higher viscosity, which is not advantageous to acquire high solid content dispersion. The particle size and PSD of the synthesized APUs are shown in Figures 1–3.

It is found that with increment of the hydrophilicity (COOH groups), smaller particle size and narrower PSD were obtained as shown in Table I and Figures 1(a)–1(d). Particle size decreased sharply at lower COOH contents while at higher COOH contents it exhibited an asymptotic behavior. As the particle size of the APU dispersion was mainly affected by the hydrophilicity.<sup>10</sup> So we can draw a conclusion that a minimum amount of ionic content is required to obtain stable dispersion. When the ionic groups reach to a certain concentration, small enough parti-

TABLE I  
Recipe of APU

APU3083	1.3	0.8	3000	51.0%	951	185	No sedimentation
APU3085	1.5	0.8	3000	50.2%	913	174	No sedimentation
APU3087	1.7	0.8	3000	50.6%	191	208	No sedimentation
APU3089	1.9	0.8	3000	50.5%	80	154	No sedimentation
APU3075	1.5	0.7	3000	51.2%	850	395	A little sedimentation
APU3095	1.5	0.9	3000	49.7%	1235	157	No sedimentation
APU3105	1.5	1.0	3000	49.2%	1422	134	No sedimentation
APU1085	1.5	0.8	1000	50.8%	40	671	Lot of sedimentation
APU2085	1.5	0.8	2000	50.2%	395	288	No sedimentation

The molar ratio of HDI to IPDI was fixed to HDI:IPDI = 30 : 70.

cle size was achieved and beyond that concentration no significant changes occurred.

Particle size decreased slightly when the NCO/OH molar ratio value was lower than 1.5. However, largest particle size was obtained when the NCO/OH molar ratio increased to 1.7. When the NCO/OH molar ratio was higher than 1.7, the particle size decreased rapidly. Figures 2(a)–2(d) showed that PSD was not so sensitive to the NCO/OH molar ratio, as the isocyanate component constitutes the hydrophobic segment and make no contribution to the dispersity.

As shown in Figures 3(a)–3(c), particle size and PSD decreased as the molecular weight  $M_n$  of the soft segment increased. This was attributed to the increase of chain flexibility. Chain flexibility affects particle size reduction because flexible particles are more deformable in a shear field, thus, at the disperse stage, the dispersed phase can be more easily broken into smaller ones.<sup>11,12</sup>

Unexpectedly, some samples showed very broad particle size distribution and tended to form bimodal. As a matter of fact, to obtain solid content higher than 55 or 60%, the particle size distribution must be either quite broad or multimodal.

From the above discussion, we can draw another conclusion that the ionic groups and soft segment length play much more important roles on determining the particle size. Visual evidence was provided by TEM micrographs as shown in Figure 4. The particles of APU based on PBA with the  $M_n$  value of 1000 and 2000 were spherical and individually dispersed in water, while particles of APU based on PBA with the  $M_n$  value of 3000 were of various forms, both in shape and size.

### Mechanical properties

All of these test films were opaque, except sample APU1085. Figure 5 shows the strain–stress curves of the APU cast films, while Table II reports the numerical values of the tensile test. We were surprised that our samples exhibited excellent mechanical properties, such as the largest elongation at break closes to 2000% and the greatest Young's modulus attained was 166.1 MPa. These materials possessed excellent properties because of the presence of Coulombic forces and the polar nature of the urethane groups in the hard segments and their ability to form hydrogen bonds. The data from Table II show that the tensile stress (say stress at 100% elongation) and the Young's modulus

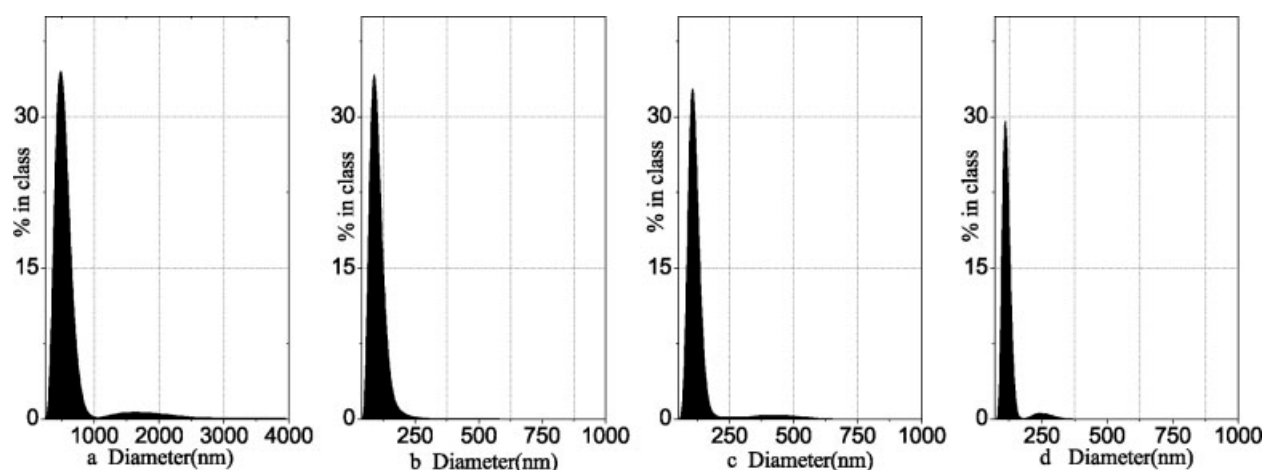
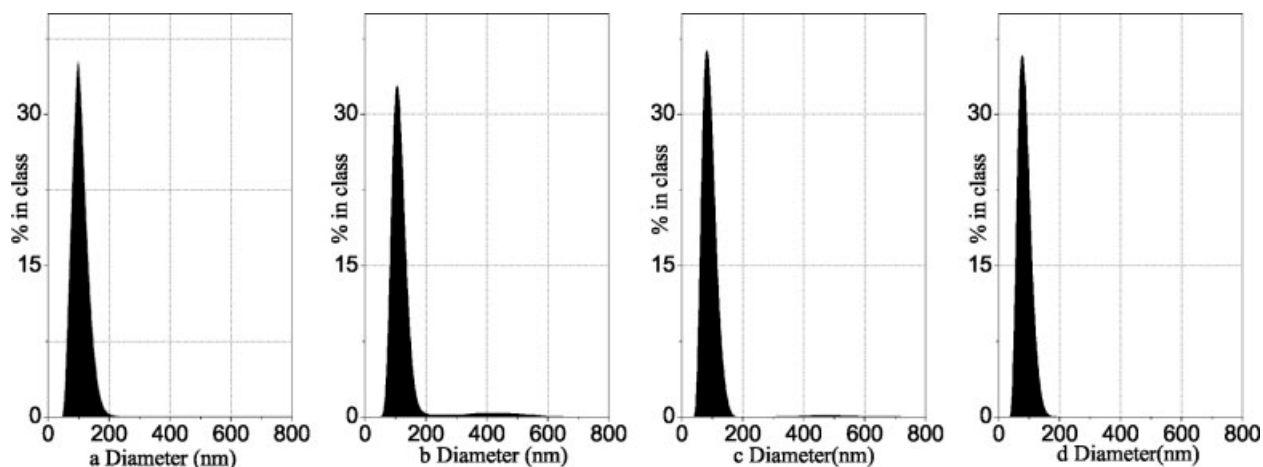


Figure 1 Particle size distribution of APU prepared from the control COOH content (%), (a) 0.7% COOH; (b) 0.8% COOH; (c) 0.9% COOH; (d) 1.0% COOH.



**Figure 2** Particle size distribution of APU prepared from the control NCO/OH molar ratio, (a) NCO/OH = 1.3; (b) NCO/OH = 1.5; (c) NCO/OH = 1.7; (d) NCO/OH = 1.9.

increased with hard segment content, as the stiffness and strength of the films were dominated by hard segment, the increment of the hard segment content gave higher intermolecular force and phase mixing.

When the  $M_n$  of the soft segment was raised, the tensile stress and the Young's Modulus increased. This was due to soft segment crystallization. Obviously, the longer soft segment gave the higher degree of crystallinity of the soft segment. APU1085 showed the poorest mechanical properties among these samples. This may be arising from very low degree of crystallinity of the soft segment.

As expected, an increment of the COOH content provoked an increase of tensile stress, and this was attrib-

uted to the Coulomb force generated by the interactive ionization among the macromolecular chains.

The stress-strain curves of the APU cast films shown in Figures 5(a)–5(c) indicated that APU1085 displayed tensile properties as an amorphous polymer, while the other samples display typical crystalline polymer tensile properties with a yield point observed. Interestingly, both APU3087 and APU3089, which possessed high hard segment content showed a secondary yield point near the 1700% elongation, thereafter the stress increased sharply until the specimen breaks. There are two explanations for this observation, one is probably faint crystallization of the hard segments, the other may be stain induced crystallization.<sup>13</sup>

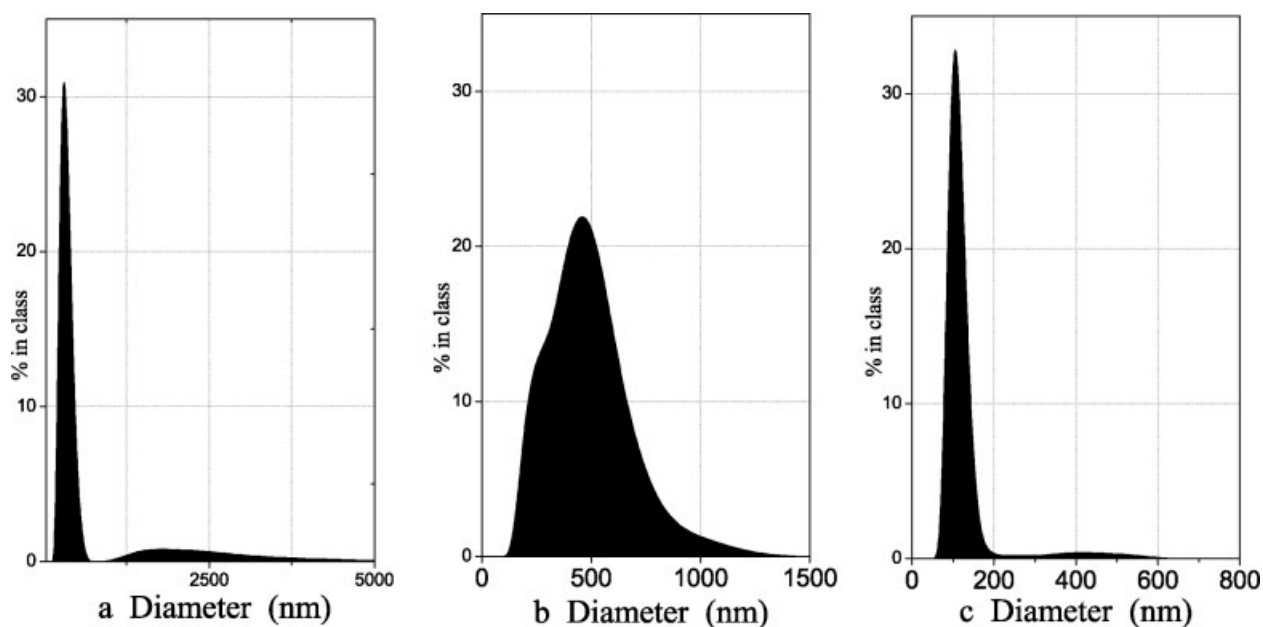


**Figure 3** Particle size distribution of APU prepared from the control  $M_n$  of PBA, (a)  $M_n = 1000$ ; (b)  $M_n = 2000$ ; (c)  $M_n = 3000$ .

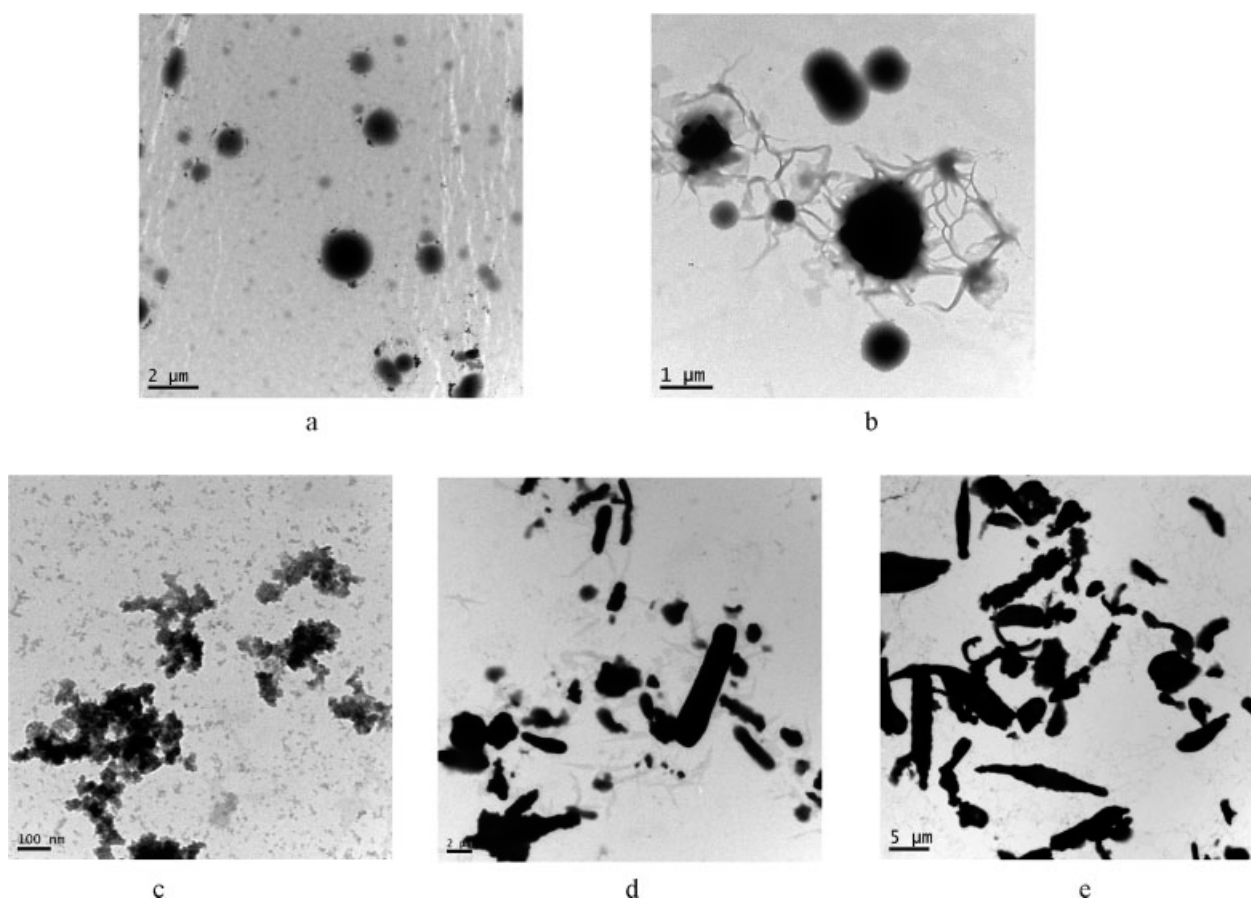


**Figure 4** TEM micrographs for APU dispersions prepared from the control of  $M_n$  of PBA and COOH content, (a) TEM Mag = 1500 $\times$ , APU1085; (b) TEM Mag = 3000 $\times$ , APU2085; (c) TEM Mag = 1500 $\times$ , APU3075; (d) TEM Mag = 3500 $\times$ , APU3085; (e) TEM Mag = 1500 $\times$ , APU3095.

### Thermal analysis

A series of DSC thermograms of APUs with soft segments of varying sequence length and with hard seg-

ments of varying concentration were given in Figure 6. The crystalline PBA polyol ( $M_n = 3000$ ) possessed the highest melting point ( $T_m = 58.02^\circ\text{C}$ ) and melt enthalpy ( $\Delta H_m = 147.20 \text{ J/g}$ ). As PBA polyol was con-

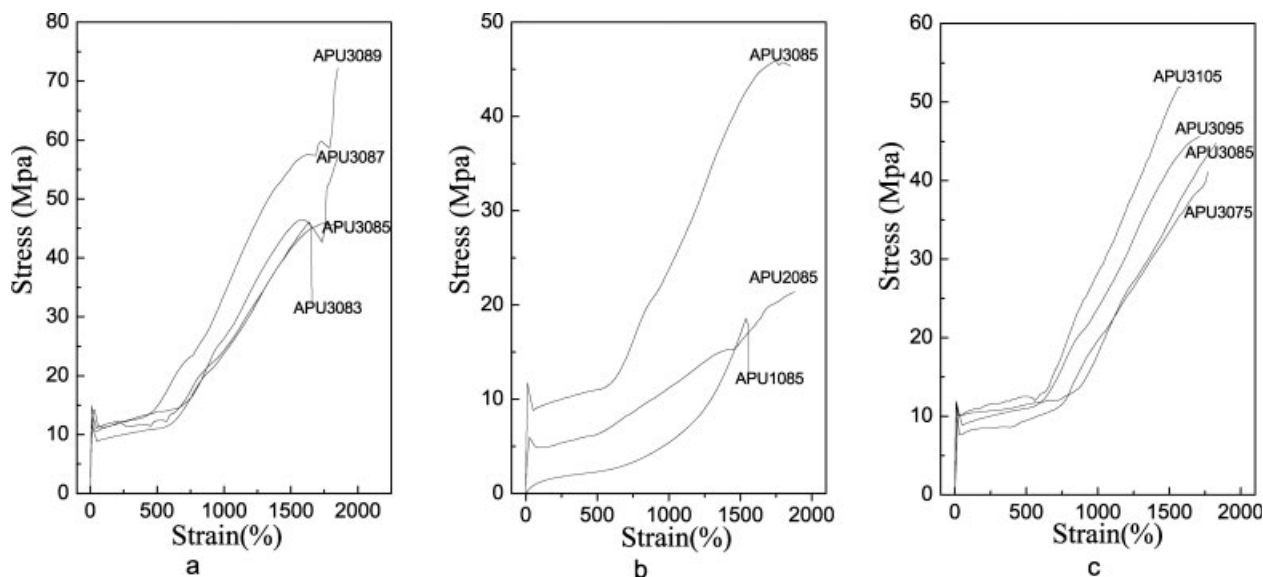


**Figure 5** Stress-strain curves of the APU cast films.

TABLE II  
The Mechanical Properties of the APU Films

Sample code	Young's modulus (MPa)	Tensile stress (Tensile strain 100%) (MPa)	Tensile stress (Tensile strain 500%) (MPa)	Tensile stress (Tensile strain 800%) (MPa)
APU3083	104.6	10.2	11.9	15.2
APU3085	108.9	8.9	10.8	17.8
APU3087	166.1	12.2	14.6	18.3
APU3089	132.3	10.9	14.7	24.2
APU1085	2.0	1.1	2.1	3.2
APU2085	60.1	5.0	6.3	9.1
APU3075	136.0	8.8	10.0	13.4
APU3095	100.7	10.7	12.5	20.4
APU3105	93.9	11.1	12.7	19.3

verted into APU, the  $T_m$  shifted to lower temperature and the  $\Delta H_m$  decreased (Table III).

An increased of hard segment concentration shifted the  $T_m$  to higher temperatures (53.54°C to 55.78°C), but the  $\Delta H_m$  become smaller. This was contrary to the results of Yen and Kuo,<sup>10</sup> Wang,<sup>14</sup> and Chen and Chang.<sup>15</sup> The decrease of  $\Delta H_m$  was because more chain extender (EDA) was required for higher NCO/OH molar ratio, resulted in more urea linkages. This will increase the compatibility of the hard and soft segment, and caused imperfect soft segments crystallization.

As shown in Figure 6, The  $T_m$  shifted to lower temperature and  $\Delta H_m$  became smaller with a decrease of the soft segment length. APU1085 which was prepared from lower  $M_n$  of PBA displayed very faint crystallization, because the shorter the soft segments give the more compatible of the hard and soft segment. As the soft segment sequence length increased, both the  $T_m$  and  $\Delta H_m$  increased. This was attributed to the greater phase separation between

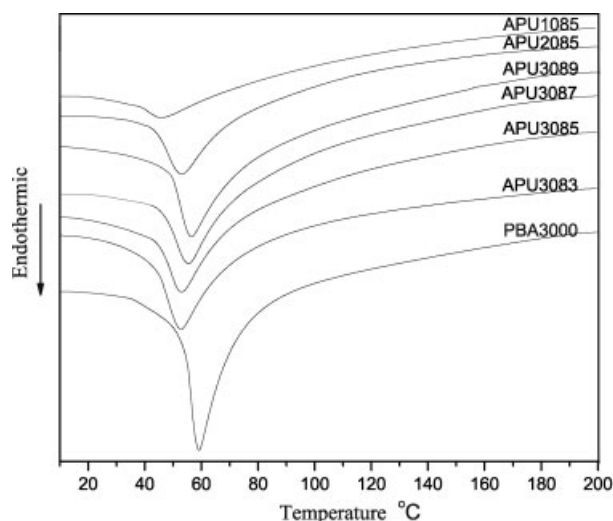


Figure 6 DSC melting thermograms of APU cast films after drying at room temperature for 7 days.

hard and soft segment, and promoting crystallization of the soft segments. On the other hand, APU1085 generated crystals that have a low degree of perfection, indicated that APU based on shorter soft segment length tends to form amorphous polymer.

### Viscoelastic properties

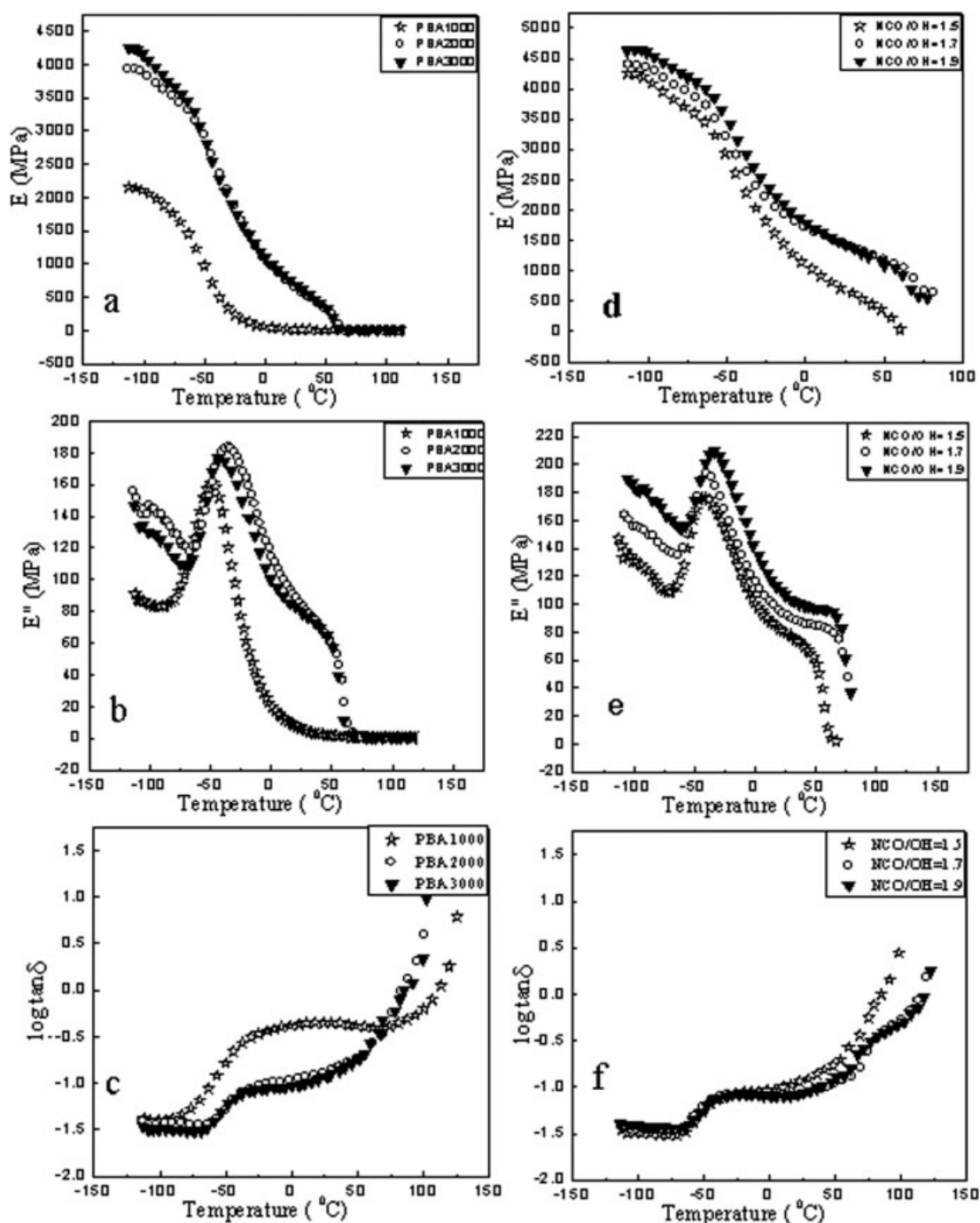
Effects of soft segment length on viscoelastic properties

Figure 7(a) showed the storage modulus ( $E'$ ) as a function of temperature ( $T$ ) of APUs containing PBA with different  $M_n$  values. The storage modulus increased with an increase of  $M_n$  of PBA in the glassy state. After passing through the glass transition region, the  $E'$  of APU1085 decreased sharply and showed a broad rubber plateau whereas APU2085 and APU3085 shifted to the entanglement region.<sup>16</sup> The two samples showed similar behavior with an upturn at about 0°C, leading to a higher value of  $E'$ . This should be related to the improvement of soft-hard phase separation and soft segment crystallization.

The loss modulus ( $E''$ ) peaks [Fig. 7(b)] at -35°C to -51°C, which corresponds to the glass transition temperature ( $T_g$ ) of the soft segment were found to decrease in this order: APU2085 > APU3085 > APU1085. Generally, the  $T_g$  of the elastomer shifts to higher temperature as the length of the soft seg-

TABLE III  
The Thermal Properties of the APUs with Various NCO/OH Molar Ratios and  $M_n$  of Soft Segment

Code	$T_m$ (°C)	$\Delta H_m$ (J/g)
PBA ( $M_n = 3000$ )	58.02	147.20
APU1085	48.89	6.47
APU2085	54.40	56.68
APU3083	53.54	118.00
APU3085	53.89	90.62
APU3087	54.91	67.16
APU3089	55.78	57.27



**Figure 7** DMA curves, (a)–(c) Effect of soft segment length ( $M_n$  of PBA) on storage modulus ( $E'$ ), loss modulus ( $E''$ ) and  $\tan \delta$ ; (d)–(f) Effect of hard segment concentration (NCO/OH molar ratio) on storage modulus ( $E'$ ), loss modulus ( $E''$ ) and  $\tan \delta$ .

ment decreased, due to the increased degree of soft-hard phase miscibility (i.e.,  $T_g$ :APU2085 > APU3085). The lowest  $T_g$  attained for APU1085 in our case could be ascribed to additional free volume associated with the chain ends of the molecules and is proportional to their concentration. The influence of the soft segment length on the glass transition properties of the APU was also emphasized in the  $\tan \delta$  curves as displayed in Figure 7(c).

Effects of hard-segment concentration on viscoelastic properties

The influence of hard segment concentration on viscoelastic properties was also investigated on a series of APU based on the same length of soft segment ( $M_n = 3000$ ). As shown in Figures 7(d) and 7(e), the storage modulus ( $E'$ ) and glass transition temperature ( $T_g$ ) increased slightly as the hard segment concentration increased. This was because the

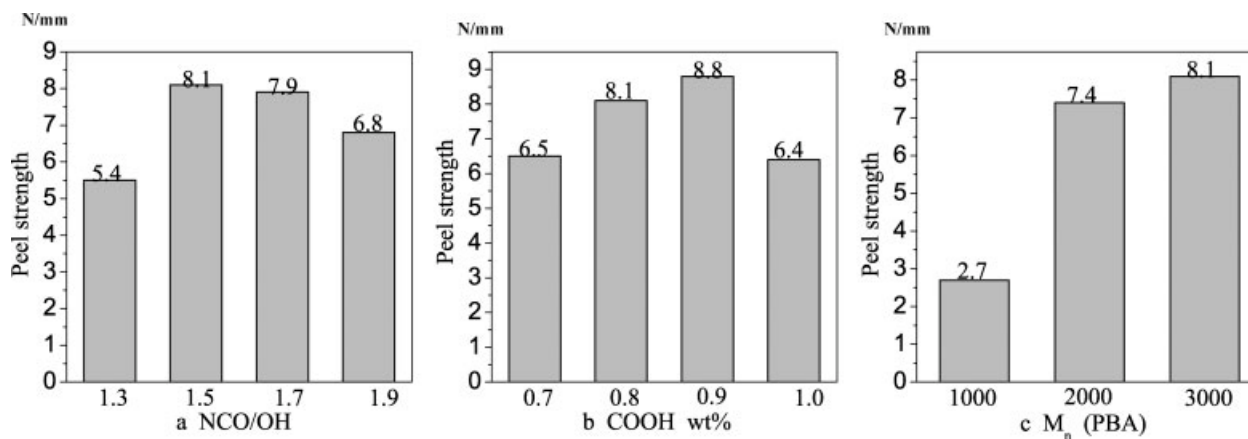


Figure 8 Effect of NCO/OH molar ratio, COOH content and  $M_n$  of PBA on peel strength.

mobility of soft segment was greatly restricted by the hard segment, which presented as filler or physical crosslinking. Another factor on  $T_g$  to be considered was the hydrogen bonding. The  $T_g$  may also be raised from the hydrogen bonding between the urethane  $N-H$  groups of the hard segment and the ester units of the soft segment.<sup>17</sup>

The loss modulus ( $E''$ ) versus temperature ( $T$ ) presented in Figure 7(e) showed that as the hard segment concentration increased, the glass transition peak shifted to higher temperature and the glass transition region broadened. However, the variation was obscure. As a matter of fact, for polymer containing longer sequence length of soft segments, the degree of interaction between the phases appears to be less pronounced. It is only at a considerable hard segment content, weight fraction between or greater than, for instance 0.4 ~ 0.6, that the glass transition temperature of soft segment is shifted to a higher temperature.<sup>18</sup>

Again, the maximal of  $\tan \delta$  peaks as shown in Figure 7(e) illustrate that differences in  $T_g$  are negligible in our case.

### Adhesive properties

The data in Figure 8 showed the effect of NCO/OH molar ratio, COOH content and  $M_n$  of soft segment on adhesive performance. Surprisingly, results showed that the synthesized APUs exhibited outstanding adhesive performance. As the hard segment content increased, the T-peel strength improved up to NCO/OH = 1.5, while it decreased slightly thereafter. The increase of peel strength with hard segment content may be arise from higher hydrogen bond density, resulted in a crosslinked network having good adhesive joint strength. However, too much hard segments probably hindered the movement of the polymer chain, and embrittled the adhesive layer of the lap joint, leading to a reduction of the peel strength.<sup>19</sup>

The peel strength increased with the ionic groups at low COOH content (0.9 wt %) can be explained by that with the increment of ionic content, more Coulomb attraction between the ionic center sites were available, and better adhesion was achieved. However, too much ionic groups in the molecular chain contribute to improvement of phase mixing between the hard and soft segments, leading to a limitation to the movement of the polymer molecular chain, which in turn causing a reduction of the peel strength.

The data from Figure 8(c) indicated that crystallization play a very important role on determining adhesive performance. Since APU1085 had very low degree of crystallinity and tended to form amorphous polymer, it presented the poorest adhesive performance. The peel strength increased with  $M_n$  of soft segment because longer soft segment usually results in higher degree of crystallinity, giving greater failure strength.

### CONCLUSIONS

Aqueous polyurethane dispersions having a solid content of about 50% were synthesized. The properties of the dispersion and its cast films were investigated by varying the COOH content, NCO/OH molar ratio and  $M_n$  of the soft segment length. The results showed that the particle size of APUs' dispersion decreased with increment of the COOH content and  $M_n$  of the soft segment, but the effect of NCO/OH molar ratio on particle size and particle size distribution was not so significant; Broad particle size distribution and bimodal were obtained for these high solid content APUs. Regarding the mechanical properties, tensile test showed that our samples exhibited excellent tensile strength and Young's modulus, the elongation at break reached to a value of 2000%. The increment of NCO/OH molar ratio and  $M_n$  of soft segment was advantageous to tensile



strength, but the effect of DMPA content on the tensile properties was insignificant. DSC and DMA analysis showed that the higher NCO/OH molar ratio yielded the higher melting temperature, as well as higher glass transition temperature. The  $T_m$  of the polymer shifted to higher temperature as the length of the soft segments increased, this can be ascribed to an increase in the degree of crystallinity. The sample prepared from PBA of 1000  $M_n$  displayed the lowest  $T_g$ , this can be explained by that the shorter soft segment length gives more additional free volume associated with the chain ends of the molecules. However, for APU containing longer soft segment length ( $M_n \geq 2000$ ), the  $T_g$  decreased with the increment of the soft segments length. T-peel strength (PVC/PVC) test results showed that the synthesized APUs possessed good adhesive performance, the maximum peel strength attained a value of 8.8 N/mm.

## References

1. Saw, L. K.; Brooks, B. W.; Carpenter, K. J.; Keight, D. V. *J Colloid Interface Sci* 2003, 257, 163.
2. Wicks, Z. W., Jr.; Wicks, D. A.; Rosthauser, J. W. *Prog Org Coat* 2002, 44, 161.
3. Lim, H.; Lee, Y.; Park, I. J.; Lee, S. B. *J Colloid Interface Sci* 2001, 241, 269.
4. Wu, L.; Chen, X.; Hu, D.; Zou, L. *Surf Interface Anal* 2001, 31, 1094.
5. Guyot, A.; Chu, F.; Schneider, M.; Graillat, C.; McKenna, T. F. *Prog Polym Sci* 2002, 27, 1615.
6. Schütze, D. I.; Kurek, G.; Rische, T.; Urban, J.; Hassel, T. U.S. Pat. 6,642,303B2 (2003).
7. Amirsakis, C. J. U.S. Pat. 6,325,887B1 (2001).
8. Temme, W.; Bergs, R.; Haberle, H.; Maier, A. U.S. Pat. Appl 2002/0004553 A1 (2002).
9. Steidl, N.; Maier, A.; Wolfertstetter, F. U.S. Pat. Appl 2005/0027092 A1 (2005).
10. Yen, M. S.; Kuo, S. C. *J Appl Polym Sci* 1998, 67, 1301.
11. Mequanint, K.; Sanderson, R. *Polymer* 2003, 44, 2631.
12. Lee, Y. M.; Lee, J. C.; Kim, B. K. *Polymer* 1994, 35, 1095.
13. Dai, X.; Xu, J.; Guo, X.; Lu, Y.; Shen, D.; Zhao, N.; Luo, X.; Zhang, X. *Macromolecules* 2004, 37, 5615.
14. Wang, X.; Luo, X.; Wang, X. *Polym Test* 2005, 24, 18.
15. Chen, S.; Chan, W. *J Polym Sci Part B: Polym Phys* 1990, 28, 1499.
16. Wiese, H. In *Polymer Dispersions and Their Industrial Applications*; Urban, D., Takamura, K., Eds.; Wiley: New York, 2002; Chapter 03, pp 63–65.
17. Schneider, N. S.; Sung, C. S. P.; Matton, R. W.; Illinger, J. L. *Macromolecules* 1975, 8, 63.
18. Seefried, C. G., Jr.; Koleske, J. V.; Critchfield, F. E. *J Appl Polym Sci* 1975, 19, 2493.
19. Desai, S. D.; Patel, J. V.; Sinha, V. K. *Int J Adhes Adhes* 2003, 23, 393.